

# DRAM1 deficiency affects the organization and function of the Golgi apparatus



Mingzhen Wei<sup>a,1</sup>, Zhou Zhu<sup>b,1</sup>, Junchao Wu<sup>a</sup>, Yan Wang<sup>a</sup>, Ji Geng<sup>a,\*</sup>, Zheng-Hong Qin<sup>a,\*</sup>

<sup>a</sup> Department of Pharmacology, Laboratory of Aging and Nervous Diseases, Jiangsu Key Laboratory of Neuropsychiatric Diseases, College of Pharmaceutical Sciences, Soochow University, Suzhou 215123, China

<sup>b</sup> Mr. and Mrs. Ko Chi Ming Centre for Parkinson's Disease Research, School of Chinese Medicine, Hong Kong Baptist University, Hong Kong, China

## ARTICLE INFO

### Keywords:

Golgi fragmentation  
DRAM1  
VSVG  
CI-MPR  
Microtubules

## ABSTRACT

DRAM1 (DNA damage-regulated autophagy modulator 1) is a transmembrane protein that predominantly localizes to the lysosome but is also found in other membranous organelles; however, its function in these organelles remains largely unknown. We found that DRAM1 was partially located in the Golgi apparatus, and knockdown of DRAM1 caused fragmentation of the Golgi apparatus in cells. The phenomenon of fragmented Golgi was not related to microtubule organization, and there was no direct interaction between DRAM1 and Golgi structural proteins (ARF1, GM130, syntaxin 6 and GRASP55). Moreover, Golgi-targeting DRAM1 failed to rescue the fragmentation of Golgi in DRAM1-deficient cells. The transport of ts045-VSVG-GFP, an indicator of movement from the Golgi apparatus to the plasma membrane, was delayed in DRAM1-knockdown cells. Moreover, the trafficking of CI-MPR from the plasma membrane to the Golgi was also impeded in DRAM1-knockdown cells. These results indicated that DRAM1 regulated the structure of the Golgi apparatus and affected Golgi apparatus-associated vesicular transport.

## 1. Introduction

The Golgi apparatus is a relatively conserved organelle consisting of several neatly stacked cisternae and vesicles of different sizes. It is composed of a *cis*-Golgi network, *medial*-Golgi network and *trans*-Golgi network that participate in protein modification, sorting and transport from the endoplasmic reticulum in the secretory pathway. The malfunction of the Golgi apparatus contributes to neurological diseases, skeletal dysplasia, skin and multi-system disorders [1]. The function of the Golgi apparatus is intimately linked to its stacked structure, and a fragmented Golgi apparatus has been observed in neurodegenerative diseases, such as Parkinson's Disease, Alzheimer's Disease and amyotrophic lateral sclerosis [2,3]. Many proteins are involved in maintaining the structure and function of the Golgi apparatus, but occasionally, we noticed a fragmented Golgi apparatus in DRAM1-knockdown cells.

DRAM1 (DNA damage-regulated autophagy modulator) is not only a p53 target gene encoding an evolutionarily conserved lysosomal

protein that induces macro-autophagy [4] but also an NF- $\kappa$ B target gene inducing selective autophagic defences against mycobacterial infection [5]. DRAM1 also promotes lysosomal membrane permeabilization and cathepsin release, which results in the mitochondria-mediated apoptosis that eliminates HIV-infected CD4<sup>+</sup> T cells [6]. In addition, DRAM1 can also promote the migration and invasion of malignant glioma stem cells [7]. Our previous research showed that DRAM1 augmented lysosomal acidification, promoted fusion between lysosomes and autophagosomes [8] and promoted apoptosis by recruiting lysosome-positioning BAX [9]. In addition, DRAM1 can also be partially localized on late endosomes, autophagosomes/autophagic lysosomes and the Golgi apparatus [10]. Whether different distributions of DRAM1 have different functions is still unclear.

In the present study, we evaluated the role of DRAM1 on the morphology of the Golgi apparatus and the functions of Golgi-mediated secretory and endocytic trafficking in DRAM1-knockdown cells. Overall, our data extended the current knowledge of DRAM1, especially regarding the maintenance of the organization of the Golgi apparatus.

**Abbreviations:** DRAM1, DNA damage-regulated autophagy modulator 1; VSVG, Vesicular stomatitis virus-glycoprotein; CI-MPR, Cation-independent mannose-6-phosphate receptor; ARF1, ADP-ribosylation factor 1; GM130, Golgi matrix protein 130 kD; GRASP55, Golgi reassembly stacking protein 2; GRASP65, Golgi reassembly stacking protein 1; ER, Endoplasmic reticulum

\* Corresponding authors at: College of Pharmaceutical Sciences, Soochow University, 199 Renai Road, Suzhou 215123, China.

E-mail addresses: [qinzhong@suda.edu.cn](mailto:qinzhong@suda.edu.cn) (Z.-H. Qin), [pharm\\_gengji@163.com](mailto:pharm_gengji@163.com) (J. Geng).

<sup>1</sup> These authors contributed equally to this paper.

<https://doi.org/10.1016/j.cellsig.2019.109375>

Received 7 May 2019; Received in revised form 7 July 2019; Accepted 26 July 2019

Available online 26 July 2019

0898-6568/ © 2019 Elsevier Inc. All rights reserved.

## 2. Materials and methods

### 2.1. Materials

MCF-7 cells were provided by Shanghai Cell Bank, Institute of Biochemistry and Cell Biology, Chinese Academy of Science. Nocodazole (M1404) and brefeldin A (203729) were procured from Sigma-Aldrich (Saint Louis, MO, USA). The DRAM1 polypeptide was synthesized by ChinaPeptides (Shanghai, China). EZ-Link™ Sulfo-NHS-Biotin (21217) was obtained from Thermo Scientific (Waltham, USA). Cycloheximide (76020-276) was purchased from Amresco (USA). The following primary antibodies were used: anti-GM130 (610,823, BD Biosciences, San Diego, CA, USA), anti-GRASP55 (10598-1-AP, Proteintech, Wuhan, China), anti-TGN46 (AHP500GT, BIO-RAD, Hercules, CA, USA), anti-GRASP65 (ab30315, Abcam, Cambridge, UK), anti-DRAM1 (ab188648, Abcam), anti-CI-MPR (ab124767, Abcam), anti-CI-MPR (ab2733, Abcam), anti-FLAG M2 (F1804, Sigma), anti- $\beta$ -actin (A2228, Sigma), anti- $\alpha$ -tubulin (Ab102, Vazyme, Nanjing, China), anti-GFP (G6539, Sigma), anti-dynein (AB1961, Millipore, USA), and ARF1 (1D9, Novus, Littleton, CO, USA). The following secondary antibodies were used: IRDye 800CW donkey anti-rabbit or anti-mouse antibodies (LI-COR Biosciences, Lincoln, NE, USA), Alexa Fluor 488 donkey anti-mouse or anti-rabbit antibodies (Life Technologies, Carlsbad, CA, USA), Alexa Fluor 555 donkey anti-mouse or anti-rabbit antibodies (Life Technologies), Cy3-Affinipure donkey anti-sheep IgG (H + L) (Jackson, USA). PrimeScript RT Master Mix (RR036A) and SYBR Premix Ex Taq (RR402A) were obtained from Takara (Japan).

### 2.2. Knockdown of DRAM1

MCF-7 cells were cultured in DMEM (Sigma) with 10% fetal bovine serum (SA015, SERANA). The sequences of DRAM1 siRNA are as follows: control siRNA (UUCUCUCCGAACGUGUCACGUTT), siDRAM1-1 (AGCCAGAUUGUACAAGATT), and siDRAM1-2 (CCACAGAAUCAAUGGUGATT). The MCF-7 cells of appropriate density were cultured in 24-well plates on the day prior to the RNAi experiment. Lipofectamine RNAiMAX reagent (0.5  $\mu$ l) was diluted with 25  $\mu$ l Opti-MEM, and gently mixed with 25  $\mu$ l Opti-MEM medium containing 40 nM siRNA. Then, the mixture was placed at room temperature for 5 min to form a siRNA/Lipofectamine RNAiMAX complex. MCF-7 cells were replaced with fresh medium and treated with the abovementioned mixture for an additional 72 h before use in experiments. The stable MCF-7 DRAM1 knockdown cells were established by lentivirus-mediated shRNA and were selected with puromycin (2  $\mu$ g/ml); the sequences of the DRAM1 shRNA are as follows: Scramble (TTCTCCGAACGTGTCACGT) and shDRAM1 (CCTACAGTCCATCATCTCTTA).

### 2.3. Plasmid transfection

The MCF-7 cells were cultured at 70–80% confluence in 24-well plates the day before transfection. Lipofectamine 2000 reagent (0.5  $\mu$ l) was diluted with 25  $\mu$ l Opti-MEM and gently blended with 25  $\mu$ l Opti-MEM containing 0.5  $\mu$ g plasmid. The mixture was placed at room temperature for 5 min and then added to the cell culture medium. The medium was changed to fresh medium after 6 h, and experiments were carried out after another 42 h.

### 2.4. Western blotting

The MCF-7 cells were harvested after treatment, lysed in RIPA lysis buffer, centrifuged at 12,000  $\times$ g for 15 min, and the protein concentration was determined using a BCA kit. SDS-PAGE was performed to separate the proteins according to their molecular weight. After electrophoresis, the proteins were transferred to a nitrocellulose membrane, and the membranes were blocked in 5% milk and incubated with primary antibodies at room temperature for 4 h. After washing in

TBST, the membranes were incubated with secondary antibodies for 1 h followed by washing in TBST, and imaging was performed with the Odyssey infrared imaging system (LI-COR Biosciences, Nebraska, USA). Quantitative analysis of the protein band intensities was performed with ImageJ.

### 2.5. RT-qPCR

Total RNA was extracted using TRIzol (Invitrogen, USA) according to the manufacturer's directions. The RNA was reverse transcribed into cDNA using the reverse transcriptase PrimeScript RT Master Mix (500 ng per 10  $\mu$ l). qPCR was carried out according to the instructions for use of SYBR Premix Ex Taq. The results were analyzed with the  $\Delta\Delta C_t$  method.

### 2.6. Immunofluorescence

The cells were fixed with 4% paraformaldehyde at room temperature for 20 min, permeated with 0.2% Triton X-100 for 15 min, blocked with 5% horse serum for 1 h, and incubated with primary antibodies overnight. After they were washed 3 times with 0.05% Triton X-100 for 10 min, the cells were incubated with secondary antibodies for 1 h at room temperature, washed three times with 0.05% Triton X-100, stained for nuclear detection with DAPI, and finally mounted with an anti-quenching liquid (F4680, Sigma). The images were obtained with a laser confocal LSM 710 microscope (Zeiss, Germany). The immunofluorescence intensity was further analyzed using Image-Pro Plus.

### 2.7. Electron microscopy

The cells were fixed overnight with 2.5% glutaraldehyde at 4 °C when the confluence reached approximately 90%, and they were scraped gently and centrifuged at low speed to collect the precipitate. The samples were sent to the electron microscopy centre at Shanghai Jiaotong University for subsequent processing and analysis.

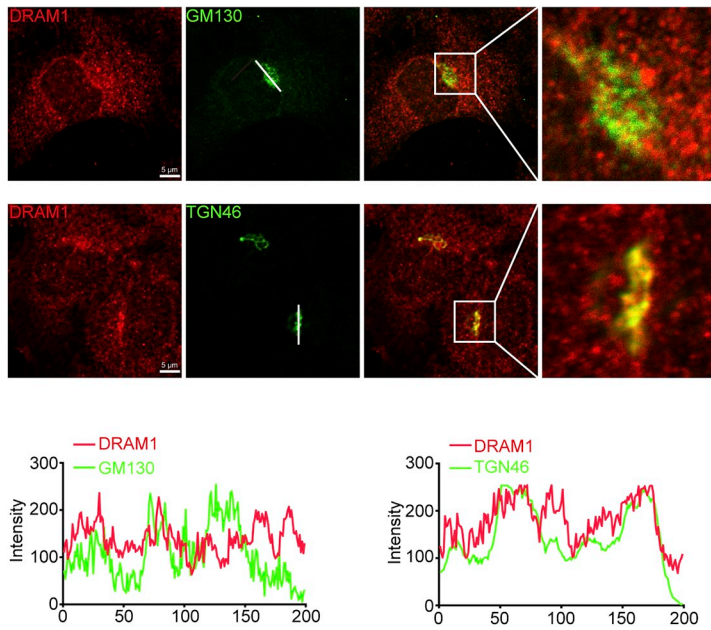
### 2.8. Ts045-VSVG-GFP transport analysis

After knockdown of DRAM1, the cells were transfected with ts045-VSVG-GFP plasmid and cultured for another 24 h. Then, the cells were transferred to 40 °C for 24 h so that the VSVG would remain in the endoplasmic reticulum. After adding cycloheximide (100  $\mu$ g/ml) 10 min in advance, the cells were cooled to 32 °C for 0, 30, 60, 90 and 120 min, and the VSVG was released from the endoplasmic reticulum to the Golgi and then to the plasma membrane. The Golgi apparatus was labelled with GRASP55 and fixed with 4% paraformaldehyde. Quantitative analysis of the VSVG transferred to the plasma membrane was performed following the biotin labelling method to extract plasma membrane VSVG.

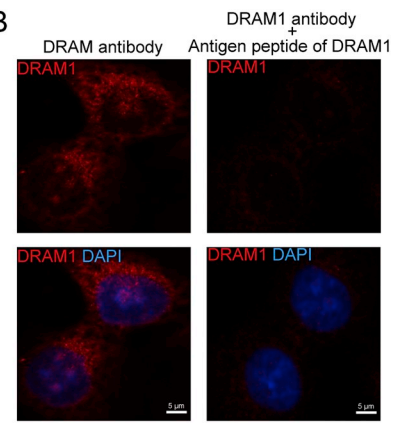
### 2.9. Detection of plasma membrane proteins

The plasma membrane proteins were isolated using sulfo-NHS-biotin-mediated biotinylation. The cells were seeded in 10-cm dishes and processed accordingly. The washed cells were centrifuged at 800  $\times$ g for 5 min and resuspended in 1 ml PBS. Each tube was added to 200  $\mu$ l of 10 mM sulfo-NHS-biotin, rotated at 4 °C for 45 min, and then centrifuged at 5000 rpm for 5 min. The precipitant was added to 1 ml PBS containing 100 mM glycine and washed three times. The precipitate was lysed with 600  $\mu$ l RIPA buffer and centrifuged at 13,500 rpm for 20 min. A portion of the supernatant was taken as total protein, and the remaining protein was added into 40  $\mu$ l avidin resin (Promega, USA) to rotate at 4 °C overnight. The beads were washed with RIPA buffer 5 times, and then the beads were boiled in 1  $\times$  loading buffer to elute the membrane proteins. The membrane proteins were detected by Western blotting.

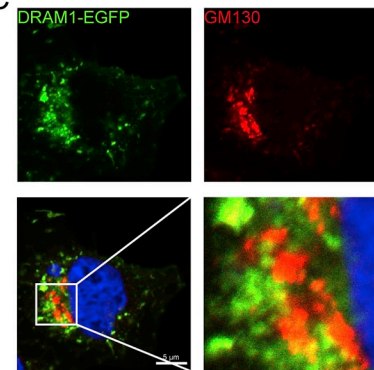
A



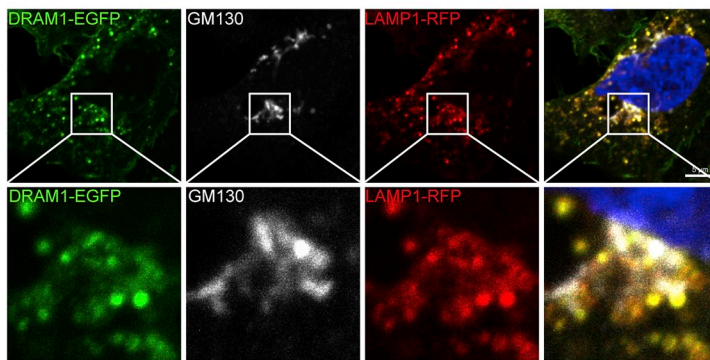
B



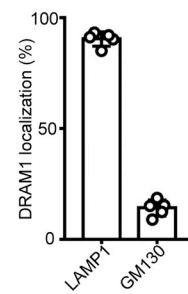
C



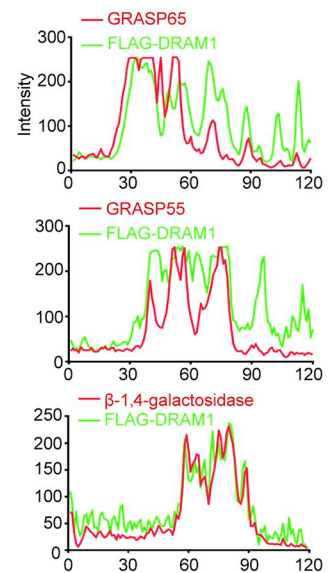
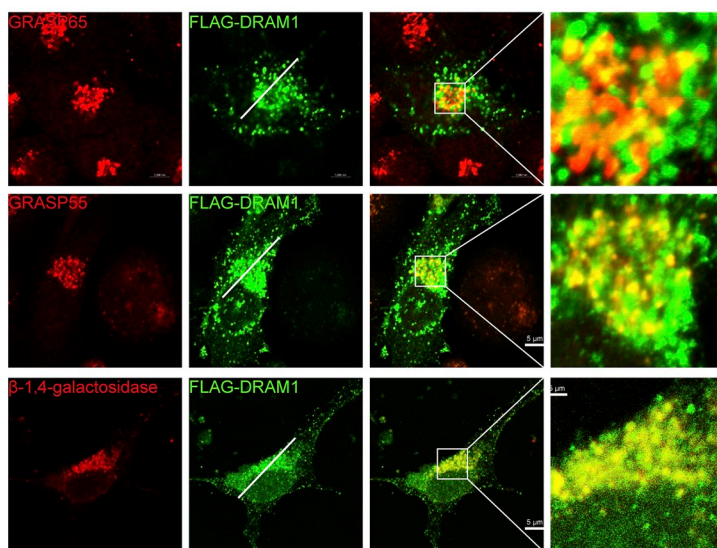
D



E



F



(caption on next page)

**Fig. 1.** A portion of cellular DRAM1 is localized in the Golgi apparatus.

(A) Cells were stained with anti-DRAM1 (red), anti-GM130 (green) and anti-TGN46 (green) antibodies. The immunofluorescence intensity was analyzed with a confocal microscopy. Scale bars: 5  $\mu$ m. (B) Test for DRAM1 immunofluorescence specificity with or without DRAM1 antigen peptide. Cells were stained with anti-DRAM1 (red) antibody and DAPI. Scale bars: 5  $\mu$ m. (C) Cells transfected with DRAM1-EGFP (green) were stained with anti-GM130 (red) to detect the co-localization of DRAM1 with the Golgi apparatus. (D) Cells transfected with DRAM1-EGFP (green) and LAMP1-RFP (red) were stained with anti-GM130 (grey) to detect the distribution of DRAM1 between the lysosome and the Golgi apparatus. (E) The ratio of DRAM1 in lysosomes and the Golgi apparatus were measured. (F) Cells were stained with anti-GRASP65 (red), anti-GRASP55 (red) and anti-FLAG (green) antibodies to detect the co-localization of exogenous DRAM1 with the Golgi apparatus. The intensity of immunofluorescence was analyzed. Scale bars: 5  $\mu$ m. (For interpretation of the references to colour in this figure legend, the reader is referred to the web version of this article.)

### 2.10. Endocytosis of CI-MPR

The cells were starved overnight with serum-free DMEM. The antibody against the extracellular domain of CI-MPR diluted with pre-cooled DMEM was added to the cells and incubated at 4 °C for 30 min; the medium was changed to normal culture medium. After 0 and 30 min, the cells were fixed with 4% paraformaldehyde for 20 min and processed for immunofluorescence as described above.

### 2.11. Co-IP

Cells were harvested, lysed with RIPA buffer on ice, centrifuged at 12,000  $\times$  g for 15 min, and 100  $\mu$ g of the protein supernatant was taken as the total protein. The pre-washed protein A/G beads were conjugated with antibodies for 4 h at 4 °C and washed 3 times with IP lysis buffer. Then, the supernatant was aspirated, and the beads were incubated with 900  $\mu$ g of fresh protein supernatant overnight. The beads were washed 5 times with IP lysis buffer and boiled after an equal volume of 2 $\times$  loading buffer was added. After centrifugation for 10 min, the supernatant was detected by Western blotting.

### 2.12. The construction of Golgi-targeting DRAM1

The Golgi targeting sequence was cloned from the sequence encoding the 81 amino acids of the N-terminal of human  $\beta$ -1,4-galactosyltransferase using Pyrobest DNA Polymerase (Takara, Japan). The sequence of sh-DRAM1 (5-CCTACAGTCCATCATCTCTTA-3) was replaced by 5-TTATTACAAAGCATTATTAGCTAT-3, which can synonymously express DRAM1 in sh-DRAM1 cells. The Golgi-targeting sequence, DRAM1 with synonymous mutations, and pcDNA3.1-EGFP-N3 were constructed by homologous recombination using a Multi One Step Cloning Kit (Yeasen, Shanghai). DRAM1-EGFP based on pcDNA3.1-EGFP-N3 was constructed as a positive control.

### 2.13. Statistical analysis

Each experiment was performed at least three times, and all bar graphs show the means  $\pm$  SD. The statistical analysis was performed using GraphPad Prism 7. The statistical analysis was obtained through unpaired *t*-tests or one-way analysis of variance (ANOVA) followed by Bonferroni's multiple comparisons. A value of  $P < .05$  was considered statistically significant.

## 3. Results

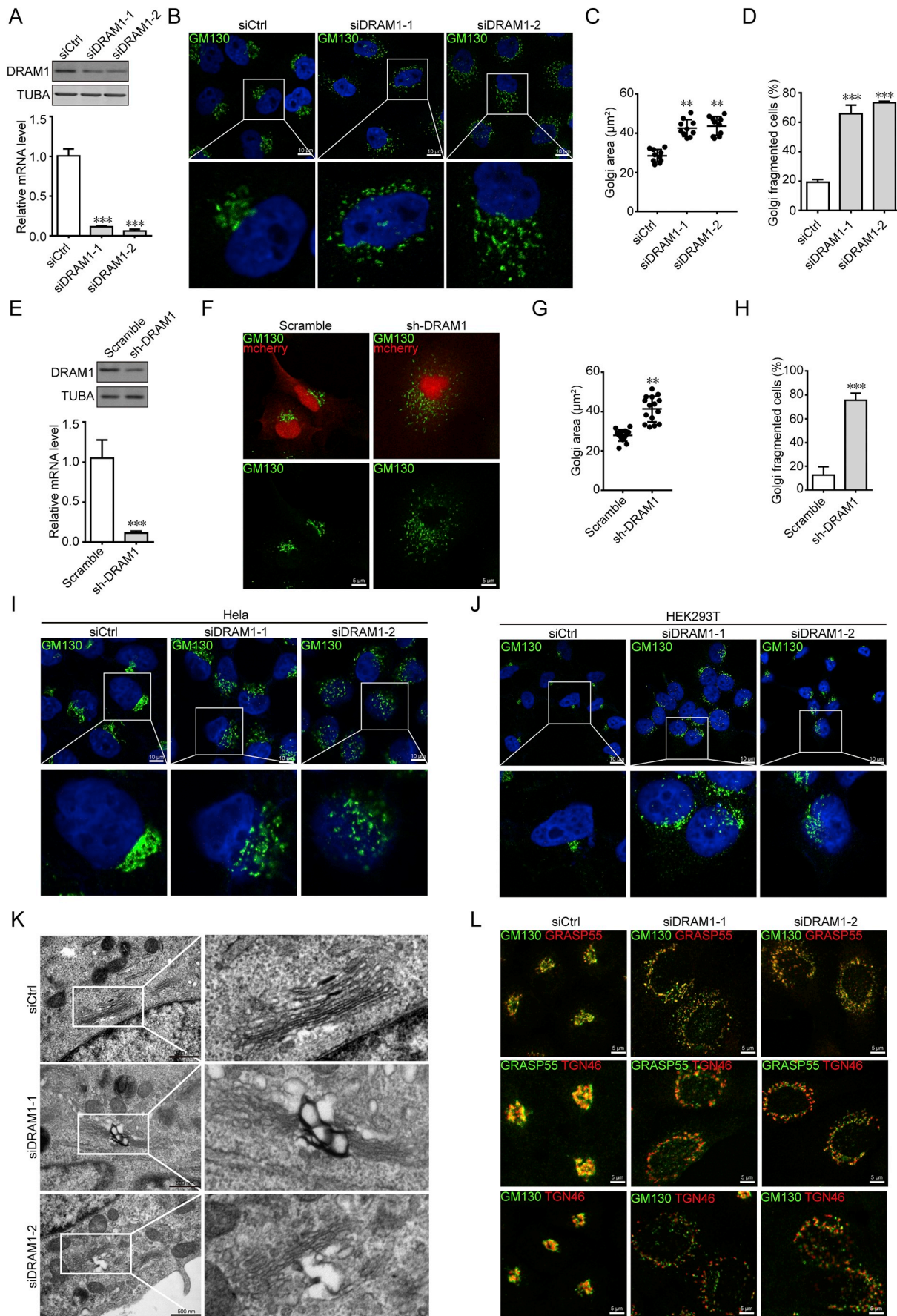
### 3.1. DRAM1 is partially localized to the Golgi apparatus

To elucidate the role of DRAM1 on membranous organelles, subcellular localization of DRAM1 in the MCF-7 cells was examined with immunofluorescence labelled antibodies against DRAM1, GM130 and TGN46. The immunofluorescence images in Fig. 1A show that endogenous DRAM1 was partially localized in the *cis*- and *trans*-Golgi, as indicated by GM130 and TGN46, respectively. To test the specificity of the DRAM1 immunofluorescence, the DRAM1 antibody was neutralized with an antigen peptide before immunofluorescence staining. As shown in Fig. 1B, the fluorescent intensity of DRAM1 was significantly

decreased when the DRAM1 antibody was adsorbed by antigen peptide, suggesting that the antibody against DRAM1 had a reasonable degree of specificity in the immunofluorescence assay. The partial co-localization between exogenous DRAM1 and endogenous GM130 also indicated that DRAM1 was partially located in the Golgi (Fig. 1C). We further tested the distribution of DRAM1 between lysosomes and the Golgi. The results in Fig. 1D-E showed that LAMP1-labelled lysosomes were partially co-localized to GM130-labelled Golgi apparatus; and 92% of DRAM1 was located in lysosomes and 15% of DRAM1 was located in the Golgi. To further assess the co-localization of DRAM1 in the Golgi apparatus, the MCF-7 cells overexpressing FLAG-DRAM1, and the *cis*-, *medial*- and *trans*-Golgi apparatuses, as indicated by GRASP65, GRASP55 and  $\beta$ -galactosidase, were detected by immunofluorescence. The results showed that the overexpressed DRAM1 was also partially localized to the Golgi apparatus (Fig. 1F).

### 3.2. Knocking down DRAM1 causes Golgi fragmentation

To examine the impact of DRAM1 on the Golgi apparatus, two different siRNAs were applied to decrease DRAM1 expression. As described in Fig. 2A, the siRNA-mediated DRAM1 knockdown exhibited a significant reduction in protein level and mRNA level, and the decrease ratio of mRNA was 89% and 94%, respectively. In contrast to control cells with a dense Golgi apparatus near the nucleus, the Golgi morphology stained by GM130 appeared fragmented in the cytoplasm in the DRAM1-knockdown cells (Fig. 2B). The results from the quantitative analysis revealed that the area of the Golgi apparatus was significantly increased, and over 70% of DRAM1-knockdown cells exhibited Golgi fragmentation (Fig. 2C and D). To further verify this phenomenon, a stable MCF-7 cell line with DRAM1 knockdown was established using lentivirus. The Western blot and RT-qPCR results showed that the sh-DRAM1 downregulated protein and mRNA level of DRAM1 (Fig. 2E). We also observed fragmentation of the Golgi structures, a finding consistent with the results observed in cells in which DRAM1 was transiently knocked down (Fig. 2F). The quantitative analysis also showed that the Golgi area was obviously increased and that approximately 80% of the Golgi was fragmented when DRAM1 was stably knocked down (Fig. 2G and H). It has been reported that altered Golgi structures were observed in cancer cells [11]. The Golgi apparatus labelled by GM130 was different in A-431 cells, U-2 OS cells and U-251 MG cells (Fig. SI-1). HeLa cells, HEK293T cells and HEK293 cells were used to detect the effect of DRAM1 on the Golgi apparatus, and the Golgi fragmentation induced by the downregulation of DRAM1 was shown to be a universal phenomenon (Fig. 2I and J, Fig. SI-2). The ultrastructure of the Golgi was further analyzed using electron microscopy. As shown in Fig. 2K, the Golgi morphology was relatively normal and had a laterally connected, elongated, flat cisternae structure in the control cells. However, the inner lumen of the Golgi was swollen in the DRAM1-knockdown cells. Because the Golgi is composed of *cis*-, *medial*- and *trans*-Golgi structures, individual organelles were stained with GM130, GRASP55 and TGN46 and detected with immunofluorescence. The results in Fig. 2L show that the whole Golgi apparatus had fallen apart in DRAM1-knockdown cells. Overall, these results demonstrated that DRAM1 was involved in maintaining the organization of the Golgi structure.



(caption on next page)

### Fig. 2. DRAM1 knockdown triggers Golgi fragmentation.

(A) Cells were transfected with siCtrl or DRAM1 siRNAs, and the protein level and mRNA level of DRAM1 were analyzed with Western blotting and RT-qPCR after 72 h.  $***P < 0.001$  versus siCtrl. (B) DRAM1-deficient MCF-7 cells were stained with anti-GM130 (green) antibody and DAPI. Scale bars: 5  $\mu$ m. (C-D) Quantitative analysis of Golgi areas ( $n = 10$ ) and the percentage of cells (100 cells) with Golgi fragmentation in (B).  $**P < 0.01$  and  $***P < 0.001$  versus siCtrl. (E) The protein content and mRNA levels of DRAM1 in scramble or sh-DRAM1 stable cell lines.  $***P < 0.001$  versus Scramble. (F) Scramble or sh-DRAM1 stable MCF-7 cells were stained with anti-GM130 (green) antibody. Scale bars: 5  $\mu$ m. (G-H) Results from the quantitative analysis of Golgi areas ( $n = 10$ ) and percentage of cells (100 cells) with Golgi fragmentation in (F).  $**P < 0.01$  and  $***P < 0.001$  versus Scramble. (I, J) The Golgi morphology in DRAM1-deficient HeLa cells and HEK293T cells. (K) The ultrastructure of Golgi in control or DRAM1 siRNA cells examined by electron microscopy. Scale bars: 500 nm. (L) The *cis*-, *medial*- and *trans*-Golgi fragmentation in the control or DRAM1 siRNA cells were stained with anti-GM130 (green), anti-GRASP55 and anti-TGN46 (red) antibodies, respectively. Scale bars: 5  $\mu$ m. (For interpretation of the references to colour in this figure legend, the reader is referred to the web version of this article.)

### 3.3. DRAM1 knockdown-mediated Golgi fragmentation is independent of microtubules and does not affect the localization of Golgi structural proteins

Microtubules are indispensable for Golgi complex assembly and maintenance. To explore the mechanisms of Golgi fragmentation caused by DRAM1 knockdown, we first investigated the changes in the cytoskeleton and found that neither microtubules nor microfilaments showed significant changes in DRAM1-knockdown cells, and they had clear filamentous structures that were similar to those of the control cells (Fig. 3A and B). To confirm that the cytoskeleton is not involved in the breakdown of the Golgi caused by DRAM1 deficiency, nocodazole, a microtubule depolymerizing agent, was used to cause microtubule depolymerization and Golgi apparatus fragmentation in our experiment, as previously reported [12]. In the present study, the microtubules were depolymerized, and the Golgi was fragmented in the cells treated with nocodazole (Fig. 3C), and the fragmentation of Golgi was not rescued by DRAM1 overexpression in these cells (Fig. 3D).

Except for with the microtubules that serve as transport roads, dynein, a minus-end-directed microtubule motor, transports numerous vesicles from the cell periphery to the perinuclear areas along the microtubules, and dynein acts on the structural integrity of the Golgi apparatus [13]. Compared to dynein in the control cells, the dynein was co-localized with the Golgi apparatus, and there were no significant changes in the level of dynein protein in DRAM1-knockdown cells, suggesting that DRAM1 had no effect on the interaction between the Golgi structure and dynein (Fig. 3E and F).

DRAM1 was partially co-localized to Golgi, and whether DRAM1 affected the structure of the Golgi apparatus through the Golgi structural proteins remained a question. Therefore, immunoprecipitation was used to detect Golgi structural proteins, namely, Arf1, GM130, STX6 and GRASP55. As presented in Fig. 3G, DRAM1 had no direct interaction with these structural proteins of the Golgi. These results suggested that DRAM1 had no direct effect on the microtubules, dynein or the structural proteins of the Golgi.

### 3.4. DRAM1 outside of the Golgi protects Golgi architecture

Golgi fragmentation is involved in several diseases, and the fragmented Golgi can be rescued in DRAM1-knockdown cells after DRAM1 overexpression (Fig. 4A). To further assess whether DRAM1 specifically maintained Golgi structure, brefeldin A, an inducer of Golgi fragmentation, was used in cells with overexpressed DRAM1 [14]. The results in Fig. 4B show that the brefeldin A treatment induced fragmentation of the Golgi structure, and the fragmentation was significantly rescued in cells overexpressing DRAM1. These results indicated that DRAM1 could protect Golgi against fragmentation. In addition, we constructed a Golgi-targeted DRAM1 plasmid to investigate the role of the DRAM1 protein that is also located in the Golgi on the maintenance of the Golgi structure (Fig. 4C). The Golgi-DRAM1-EGFP plasmid was transfected into the stable DRAM1-deficient cells to observe whether it could rescue the fragmentation of Golgi. In the control cells, the Golgi-DRAM1-EGFP co-localized with the Golgi apparatus, indicating that the plasmid was constructed successfully. Overexpressing DRAM1-EGFP can rescue the Golgi fragmentation in DRAM1-knockdown cells; however, the Golgi-DRAM1-EGFP failed to rescue the Golgi fragmentation (Fig. 4D).

Similarly, RAM1-EGFP can protect the Golgi against fragmentation induced by brefeldin A; but the Golgi-DRAM1-EGFP did not rescue the Golgi fragmentation (Fig. 4E). These results indicated that DRAM1 outside of the Golgi protected and maintained the Golgi architecture.

### 3.5. DRAM1 knockdown blocks the transport of ts045-VSVG-GFP from the Golgi to the plasma membrane

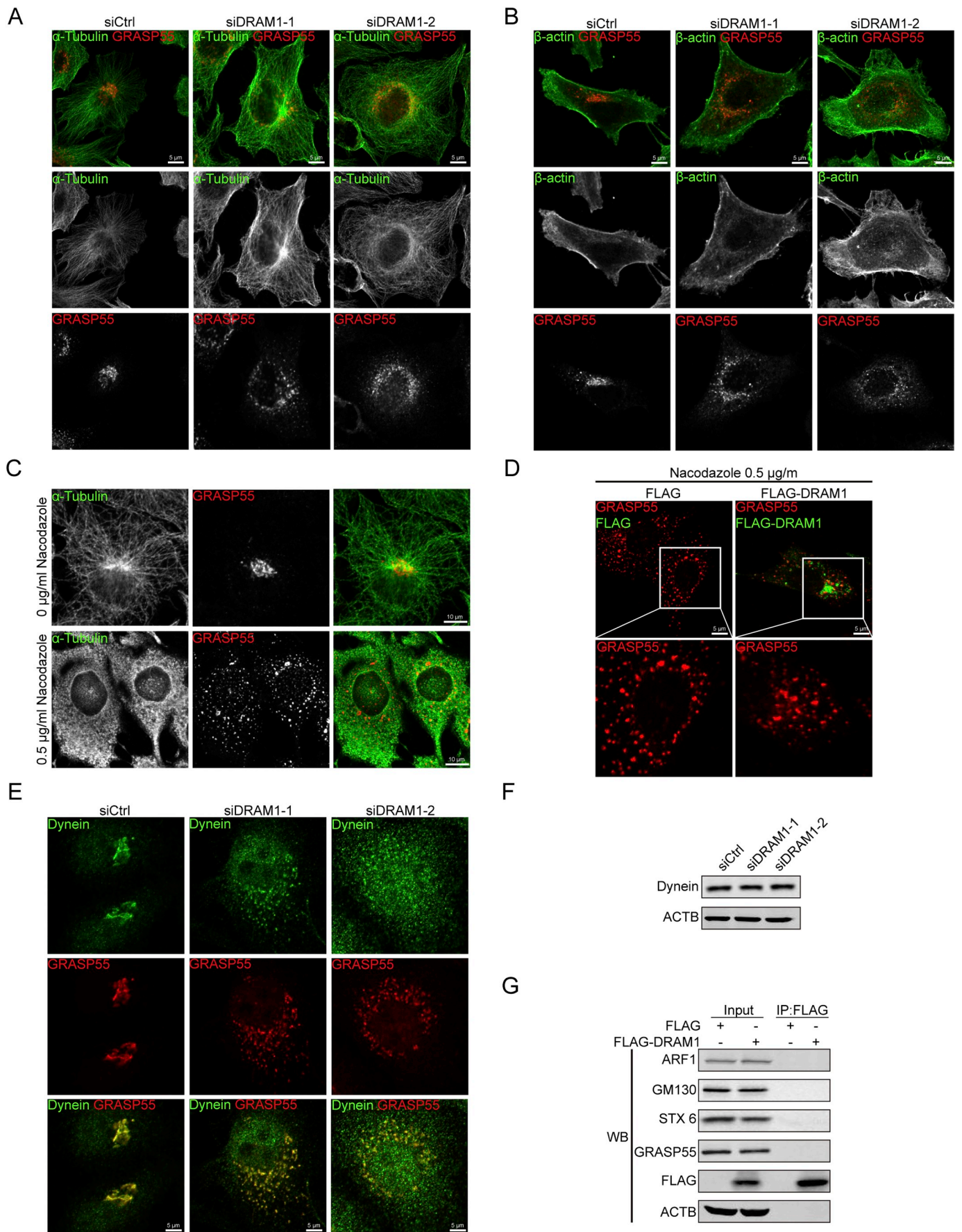
The Golgi is critical for vesicular trafficking; therefore, we examined whether impairment of Golgi trafficking occurred following the depletion of DRAM1. Ts045-VSVG-GFP is generally used as a tracer to visualize substance transport along the endoplasmic reticulum-Golgi apparatus-plasma membrane (ER-Golgi-PM) axis [15,16]. The cells were transfected with ts045-VSVG-GFP, and when the cells were shifted to the non-permissive temperature of 40 °C overnight, the misfolded ts045-VSVG-GFP was retained in the endoplasmic reticulum. When the cells were shifted to the permissive temperature of 32 °C, at different time points, ts045-VSVG-GFP was transported to the Golgi apparatus and then to the plasma membrane. In the control cells, after the cells were kept at 32 °C, the ts045-VSVG-GFP localized to the ER in 0 min (Fig. 5A); it reached the Golgi within 30–60 min (Fig. 5B and C) and reached the plasma membrane within 90–120 min (Fig. 5D and E). In the DRAM1-knockdown cells, consistent with the control, the ts045-VSVG-GFP was retained in the ER at 0 min (Fig. 5A) and moved to the Golgi apparatus within 30–60 min (Fig. 5B and C); however, the ts045-VSVG-GFP accumulated in the Golgi with no apparent movement towards the plasma membrane at 90–120 min (Fig. 5D and E).

We further pulled down biotin-labelled cell membrane proteins using an avidin-biotin binding assay to quantify the trafficking of ts045-VSVG-GFP to the plasma membrane. In the control cells, the protein level of ts045-VSVG-GFP on the plasma membrane increased continuously from 0 to 120 min, and approximately 96% of the ts045-VSVG-GFP reached the plasma membrane. In the DRAM1-knockdown cells, the amount of ts045-VSVG-GFP transported to the plasma membrane was relatively low compared to the control cells. The quantitative results showed that only 38% of the ts045-VSVG-GFP was transported to plasma membrane (Fig. 5F and G). These results indicated that, consistent with the structural abnormality of the Golgi apparatus, trafficking from the Golgi to the plasma membrane was delayed after depletion of DRAM1.

### 3.6. DRAM1 knockdown perturbs the transport of CI-MPR from the plasma membrane to the Golgi

As a receptor localized to the *trans*-Golgi and needed for transporting lysosomal acidic hydrolase with mannose-6-phosphate from the TGN for uptake by the endosomal-lysosomal system, CI-MPR can also be found in the plasma membrane where it captures mannose 6-phosphate tagged enzymes [17]. As shown in Fig. 6A, the CI-MPR was dispersed in the cytoplasm in the DRAM1-knockdown cells with fragmented Golgi structures, and while in control cells, it was collected in the perinuclear region. Additionally, the ratio of the CI-MPR in the plasma membrane was significantly increased in DRAM1-knockdown cells compared to the control cells (Fig. 6B).

To determine whether endocytosis from the plasma membrane to



(caption on next page)

**Fig. 3.** DRAM1 has no remarkable influence on the morphology of microtubules and some Golgi structural proteins. (A-B) The cells were transfected with siCtrl or DRAM1 siRNAs for 72 h and then stained with anti- $\alpha$ -tubulin and anti-GRASP55 antibodies, or anti- $\beta$ -actin and anti-GRASP55 antibodies. Scale bars: 5  $\mu$ m. (C) Cells were treated with nocodazole (0.5  $\mu$ g/ml) for 2 h and then stained with anti- $\alpha$ -tubulin and anti-GRASP55 antibodies. Scale bars: 5  $\mu$ m. (D) The cells were transfected with FLAG or FLAG-DRAM1 for 36 h and then treated with nocodazole (0.5  $\mu$ g/ml) for another 2 h, and then, cells were fixed and stained with anti-FLAG and anti-GRASP55 antibodies. Scale bars: 5  $\mu$ m. (E) The cells were transfected with siCtrl or DRAM1 siRNAs for 72 h and then stained with anti-dynein and anti-GRASP55 antibodies. Scale bars: 5  $\mu$ m. (F) The protein level of dynein after cells were transfected with siCtrl or DRAM1 siRNA. (G) Western blot analysis of endogenous ARF1, GM130, syntaxin 6 and GRASP55 after immunoprecipitation by DRAM1.

the Golgi was blocked or not, the CI-MPR on the cell surface was marked with an anti-CI-MPR antibody in its extracellular region, and the co-localization of the CI-MPR and Golgi apparatus was detected using immunofluorescence. The results, as shown in Fig. 6C and D, revealed that the co-localization between the surface CI-MPR and Golgi was downregulated in the DRAM1-knockdown cells relative to control cells 30 min after endocytosis was initiated. These results suggested that CI-MPR-mediated endocytosis from the cell surface to the Golgi was impaired after DRAM1 was knocked down.

#### 4. Discussion

This study provides insights into a possible role of DRAM1 in the structure and function of the Golgi during vesicular transport. The Golgi apparatus in mammalian cells has a unique architecture. Under confocal microscopy, the Golgi apparatus is located around the nucleus and shows a series of long ribbon-like membranes tightly packed together. Under electron microscopy, it consists of neatly stacked cisternae and vesicles of various size. The fragmented Golgi is an early marker of apoptosis in neurodegenerative diseases such as ALS and AD [18,19] and is also an important hallmark of cancers [11]. Restoration of the stacked Golgi morphology dramatically inhibited breast cancer cell invasion [20]. Moreover, fragmented and scattered Golgi are always observed in cells stimulated with alcohol, amyloid  $\beta$ , tau, and apoptosis inducer, and during nocodazole-induced microtubule depolymerization [21–25]. In addition, decreased Golgi structural proteins such as p115, syntaxin 5, GRASP65, GM130 and giantin can disturb the Golgi structure [26,27]. Previous studies have shown that DRAM1 is decreased in several cancer cells and can be detected in the Golgi apparatus [4,10]. Although the correlation between Golgi fragmentation and DRAM1 expression in cancers remains unclear, our results showed that, as a downregulated protein in cancers, DRAM1 depletion resulted in dispersed Golgi, which is a universal phenomenon of different cells.

As a dynamic organelle, the Golgi has a structure that depends mainly on maintenance by three types of proteins, including microtubules and microtubule-based motors, Golgi structural proteins, and vesicular transport proteins. The stacking factors p115, GM130, Golgin84 and Giantin maintain the morphology of the Golgi apparatus [28]. GRASP55 (Golgi reassembly stacking protein of 65 kDa) and GRASP65 in the Golgi matrix are also involved in the stacking of Golgi cisternae and the connection between the Golgi ribbons [29,30]. COP II (coatamer protein complex II) and COP I, constituted by ARF1 and a coatamer, are important complexes involved in the transport between the ER and the Golgi apparatus [31]. Moreover, dynein and dynactin are microtubule-based motors that transport vesicles exclusively to the microtubule minus end near the nuclear envelope, while kinesin drives vesicles exclusively towards the microtubule plus end [32]. Unfortunately, DRAM1 had no direct interaction with some Golgi structural proteins, and DRAM1 out of the Golgi preserved Golgi morphology against fragmentation. Additionally, it is also noteworthy that the depletion of 159 signalling genes by an RNAi screen also impaired Golgi morphology [33], indicating that the structural maintenance of the Golgi is regulated by many factors. Therefore, the concrete mechanism of DRAM1 to maintain the Golgi apparatus needs to be further studied.

The Golgi is responsible for modifying proteins and lipids into functional molecules and sorting them to specific intracellular or extracellular destinations. The *cis*-Golgi mainly receives proteins and

lipids from the ER, and these cargoes are processed and mainly glycosylated by the Golgi in the medial cisternae and transported to the *trans*-Golgi. In the *trans*-Golgi, vesicles carrying various substances are packaged and sorted for destination in the endosomal-lysosomal system or the plasma membrane. O-glycans and N-glycans signal apical sorting that results in the assignment of diverse functions and different sorting pathways. O-glycoproteins mainly exist in mucus and immunoglobulins. For instance, *N*-acetylgalactosamine (GalNAc) is added to mucins by UDP-*N*-acetylgalactosamine-polypeptide *N*-acetylgalactosaminyl-transferases (ppGalNTases) in the Golgi to generate many mature mucins that exhibit different O-glycan structures [34]. Regarding N-glycosylation, the enzyme  $\beta$ -1,4-galactosyltransferase 1 ( $\beta$ 4GalT1) is a *trans*-Golgi resident enzyme that transfers galactose from UDP-galactose to the *N*-acetylglucosamine ( $\beta$ -GlcNAc) acceptor in the glycan molecules containing a non-reducing end. Deficiency of  $\beta$ 4GalT1 causes a congenital disorder of glycosylation characterized by hydrocephalus, myopathy, and blood-clotting defects [35]. The Golgi apparatus can also regulate autophagy. RAB2 (member RAS oncogene family 2A) resided primarily in the Golgi apparatus can be dissociated from Golgi to interact with ULK1 complex after autophagy stimulation, which facilitates the recruitment of ULK1 complex to form phagophores [36]. Under short-term glucose deprivation-induced autophagy, a subpopulation of the Golgi stacking protein GORASP2/GRASP55 is targeted from the Golgi to the interface between autophagosomes and lysosomes to promote autophagosome maturation [37].

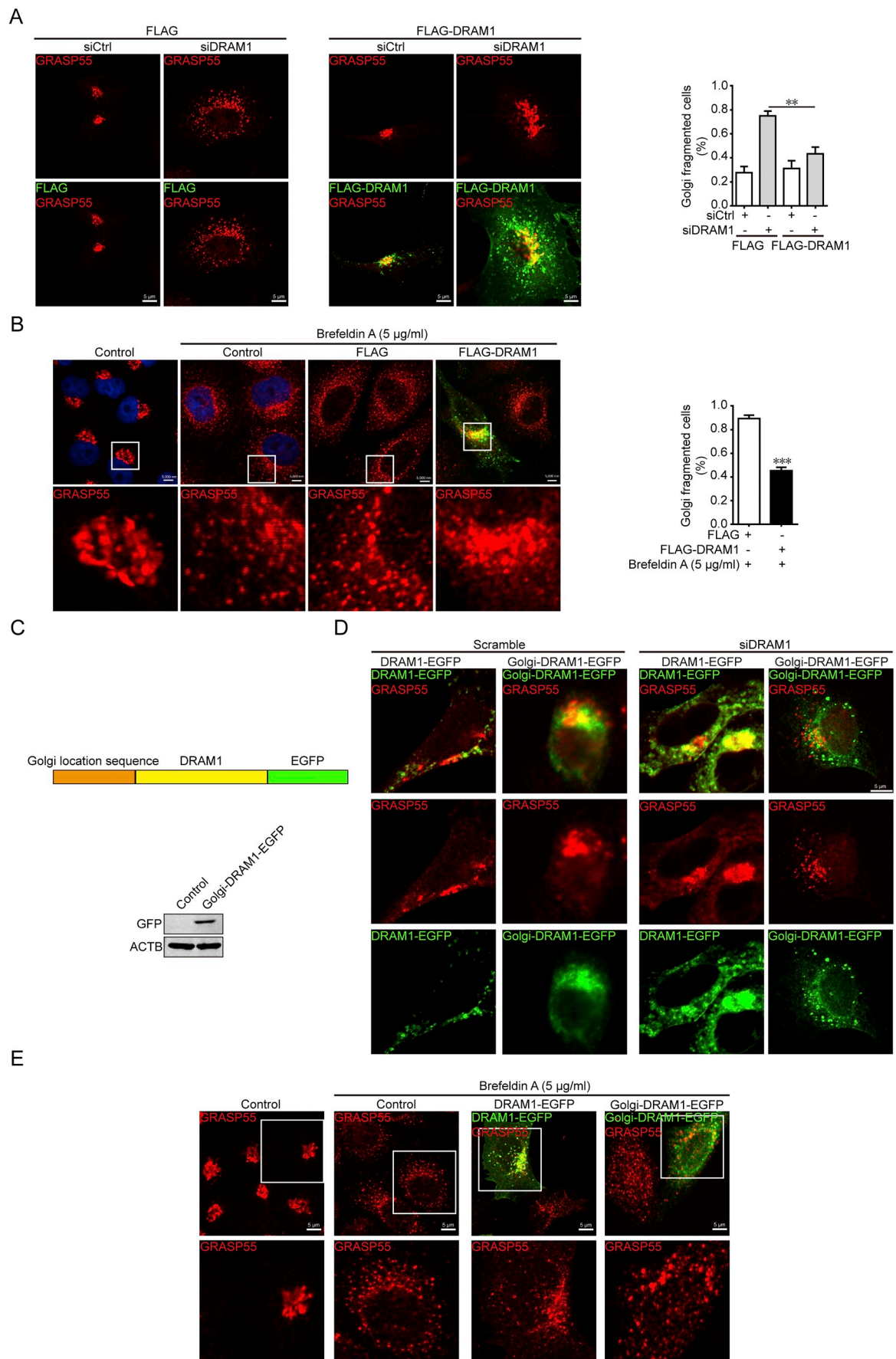
Ts045-VSVG-GFP and CI-MPR were used to monitor the exo/endocytic traffics. CI-MPR is a receptor mainly located with mannose 6-phosphate in the *trans*-Golgi apparatus to modify acidic hydrolase [38]. Because of incorrect sorting, a small portion of the CI-MPR in the cell is transported from the TGN to the plasma membrane [39]. The increase in surface CI-MPR also suggested disordered Golgi in the DRAM1-knockdown cells. Considering the downregulated secretory pathway, we speculated that decreased endocytic traffic was also responsible for the increased ratio of surface CI-MPR, and found that transport was impeded. These results revealed that vesicle trafficking was influenced, to some extent, in DRAM1-knockdown cells with fragmented Golgi. Moreover, endocytosis is involved in early endosomes, multivesicular bodies, late endosomes and lysosomes, but how DRAM1 affects this process remains unclear.

In conclusion, the present data demonstrated that a portion of DRAM1 was partially localized in the Golgi apparatus, and it preserved Golgi morphology and maintained vesicle trafficking between the Golgi apparatus and plasma membrane (summarized in Fig. 7) in a manner independent of the microtubules, microfilaments and Golgi-located DRAM1. Golgi fragmentation and DRAM1 downregulation are hallmarks that have been reported in cancers. Therefore, further work needs to be done to explore the correlation between Golgi fragmentation and DRAM1 expression in cancers, the concrete mechanism of DRAM1 in regulating the Golgi apparatus and the function of Golgi-located DRAM1 in specific disorders.

Supplementary data to this article can be found online at <https://doi.org/10.1016/j.cellsig.2019.109375>.

#### Consent for publication

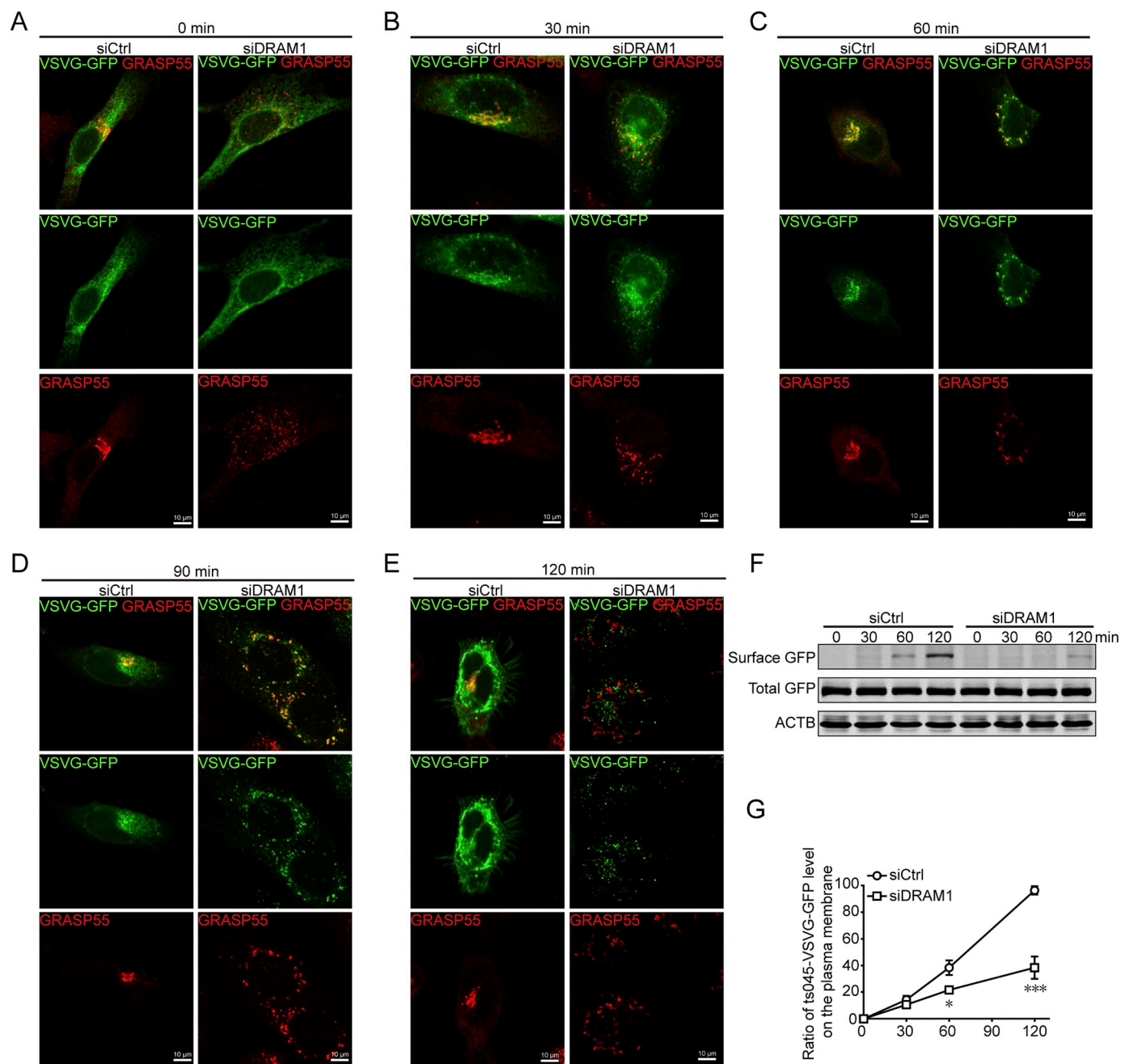
All authors read and are consent for the publication of the manuscript.



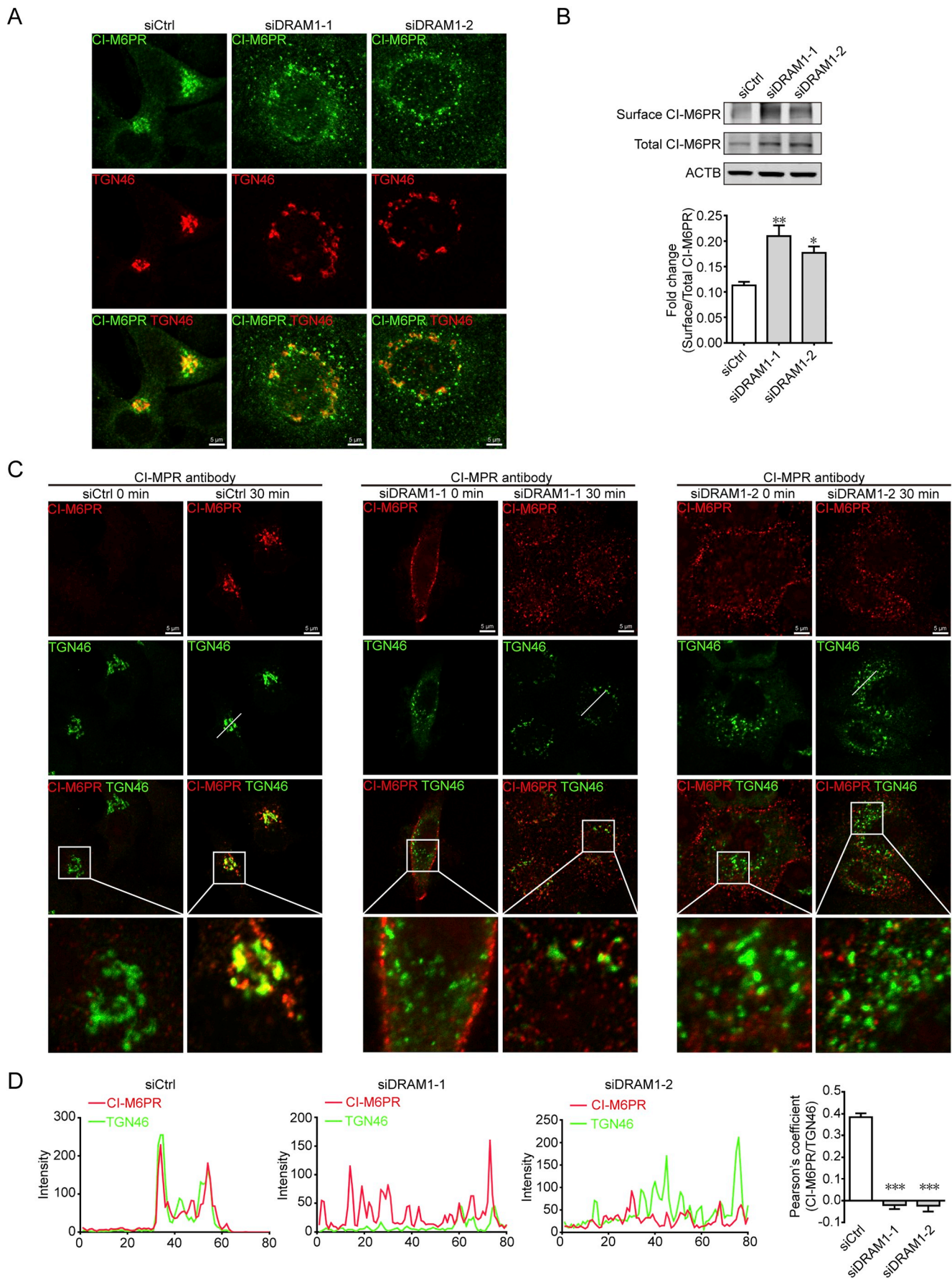
(caption on next page)

**Fig. 4.** DRAM1 outside the Golgi maintains the morphology of Golgi.

(A) The cells were treated with siCtrl or DRAM1 siRNA for 48 h and then transfected with FLAG or FLAG-DRAM1. Cells were stained with anti-FLAG and anti-GRASP55 antibodies. The result of the quantitative analysis is shown as the average percentage of cells with Golgi fragmentation.  $n = 100$ ,  $^{**}P < 0.01$  versus siDRAM1 + FLAG. Scale bars: 5  $\mu\text{m}$ . (B) The cells were transfected with FLAG or FLAG-DRAM1 for 36 h and then treated with brefeldin A (5  $\mu\text{g}/\text{ml}$ ) for another 1 h and stained with anti-FLAG and anti-GRASP55 antibodies.  $n = 100$ ,  $^{***}P < 0.001$  versus FLAG + brefeldin A. Scale bars: 5  $\mu\text{m}$ . (C) The construction and expression of the Golgi-targeting DRAM1 plasmid (Golgi-DRAM1-EGFP). (D) Scramble and sh-DRAM1 in stable cell lines were transfected with Golgi-DRAM1-EGFP for 36 h, and then, the cells were stained with anti-GRASP55 antibody. Scale bars: 5  $\mu\text{m}$ . (E) The cells were transfected with Golgi-DRAM1-EGFP for 36 h and then treated with brefeldin A (5  $\mu\text{g}/\text{ml}$ ) for an additional 1 h. The cells were stained with anti-GRASP55 antibody. Scale bars: 5  $\mu\text{m}$ .

**Fig. 5.** DRAM1 knockdown delays the trafficking of ts045-VSVG-GFP from the Golgi to the plasma membrane.

(A–E) The cells were treated with siCtrl or DRAM1 siRNA for 48 h, transfected with ts045-VSVG-GFP for 24 h, and incubated at 40  $^{\circ}\text{C}$  for 24 h. After incubation, the cells were cooled to 32  $^{\circ}\text{C}$  for 30 min, 60 min, 90 min and 120 min. At the indicated times, the cells were fixed and stained with anti-GRASP55 (red). Scale bars: 5  $\mu\text{m}$ . (F) The plasma membrane proteins were labelled with biotin reagent and then immunoprecipitated with avidin-resin. Western blot analysis of the ts045-VSVG-GFP on the plasma membrane after the temperature was decreased from 40  $^{\circ}\text{C}$  to 32  $^{\circ}\text{C}$  at various times. (G) The ratio of ts045-VSVG-GFP on the plasma membrane to the total GFP in the control and DRAM1 siRNA cells.  $n = 3$ ,  $^{*}P < 0.05$  and  $^{***}P < 0.001$  versus siCtrl. (For interpretation of the references to colour in this figure legend, the reader is referred to the web version of this article.)



(caption on next page)

**Fig. 6.** The distribution and trafficking of CI-MPR is perturbed with Golgi fragmentation.

(A) The cells were transfected with control or DRAM1 siRNAs for 72 h and then stained with anti-CI-MPR (green) and anti-TGN46 (red) antibodies. Scale bars: 5  $\mu$ m. (B) The Western blot analysis and ratio of CI-MPR on the cell surface in the control and DRAM1 siRNA cells.  $n = 3$ ,  $^*P < 0.05$  and  $^{**}P < 0.01$  versus siCtrl. (C) The results of the analysis of the transport of CI-MPR from the cell surface to the Golgi. The control and DRAM1 knockdown cells were incubated with 10  $\mu$ g/ml CI-MPR antibody for 30 min at 4  $^{\circ}$ C followed by incubation at 37  $^{\circ}$ C for 30 min. Next, the cells were fixed and stained with anti-TGN46 antibody. Scale bars: 5  $\mu$ m. (D) The immunofluorescence intensity of CI-MPR (red) and TGN46 (green) were analyzed. The Pearson's correlation coefficient was determined in ImageJ software and used to further quantify the co-localization of endocytotic CI-MPR and TGN46.  $n = 3$ ,  $^{***}P < 0.001$  versus siCtrl. (For interpretation of the references to colour in this figure legend, the reader is referred to the web version of this article.)

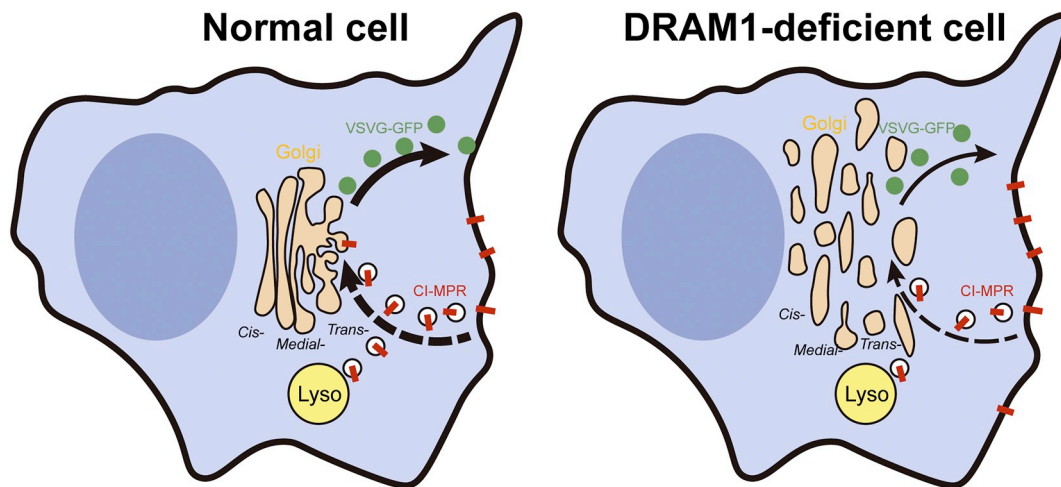


**Fig. 7.** A schematic depiction of the effects of DRAM1 on the morphology and function of the Golgi apparatus.

Decreased expression of DRAM1 triggers the fragmentation of the Golgi apparatus, leading to reduced vesicle trafficking between the Golgi apparatus and plasma membrane.

#### Authors' contributions

MZW and ZZ performed the experiments; JCW and YW prepared materials during experiments; JG and ZHQ designed the experiment, analyzed the data and wrote the manuscript. All authors read and approved the final manuscript.

#### Declaration of Competing Interest

All authors declare no conflict of interest.

#### Acknowledgements

This work was supported by grants from the National Natural Science Foundation of China (Grant No. 81730092 for ZHQ, Grant No. 81671252 for YW) and the Priority Academic Program Development of the Jiangsu Higher Education Institutes (PAPD).

#### References

- [1] M. Bexiga, J. Simpson, Human diseases associated with form and function of the Golgi complex, *Int. J. Mol. Sci.* 14 (9) (2013) 18670–18681.
- [2] Y. Fujita, E. Ohama, M. Takatama, S. Al-Sarraj, K.J.A.n. Okamoto, Fragmentation of Golgi apparatus of nigral neurons with  $\alpha$ -synuclein-positive inclusions in patients with Parkinson's disease, *Acta Neuropathol.* 112 (3) (2006) 261–265.
- [3] N. Gonatas, J.O. Gonatas, A.J.H. Stieber, c. biology, The involvement of the Golgi apparatus in the pathogenesis of amyotrophic lateral sclerosis, Alzheimer's disease, and ricin intoxication, *Histochem. Cell Biol.* 109 (5–6) (1998) 591–600.
- [4] D. Crighton, S. Wilkinson, J. O'Prey, N. Syed, P. Smith, P.R. Harrison, M. Gasco, O. Garrone, T. Crook, K.M. Ryan, DRAM, a p53-induced modulator of autophagy, is critical for apoptosis, *Cell* 126 (1) (2006) 121–134.
- [5] M. van der Vaart, C.J. Korbbe, G.E. Lamers, A.C. Tengeler, R. Hosseini, M.C. Haks, T.H. Ottenhoff, H.P. Spaik, A.H. Meijer, The DNA damage-regulated autophagy modulator DRAM1 links mycobacterial recognition via TLR-MYD88 to autophagic defense [corrected], *Cell Host Microbe* 15 (6) (2014) 753–767.
- [6] M. Laforge, S. Limou, F. Harper, N. Casartelli, V. Rodrigues, R. Silvestre, H. Haloui, J.F. Zagury, A. Senik, J. Estaquier, DRAM triggers lysosomal membrane permeabilization and cell death in CD4(+) T cells infected with HIV, *PLoS Pathog.* 9 (5) (2013) e1003328.
- [7] S. Galavotti, S. Bartesaghi, D. Faccenda, M. Shaked-Rabi, S. Sanzone, A. McEvoy, D. Dinsdale, F. Condorelli, S. Brandner, M. Campanella, R. Grose, C. Jones, P. Salomoni, The autophagy-associated factors DRAM1 and p62 regulate cell migration and invasion in glioblastoma stem cells, *Oncogene* 32 (6) (2013) 699–712.
- [8] X.D. Zhang, L. Qi, J.C. Wu, Z.H. Qin, DRAM1 regulates autophagy flux through lysosomes, *PLoS One* 8 (5) (2013) e63245.
- [9] J.J. Guan, X.D. Zhang, W. Sun, L. Qi, J.C. Wu, Z.H. Qin, DRAM1 regulates apoptosis through increasing protein levels and lysosomal localization of BAX, *Cell Death Dis.* 6 (2015) e1624.
- [10] L.Y. Mah, J. O'Prey, A.D. Baudot, A. Hoekstra, K.M. Ryan, DRAM-1 encodes multiple isoforms that regulate autophagy, *Autophagy* 8 (1) (2012) 18–28.
- [11] A. Petrosyan, Onco-Golgi: is fragmentation a gate to Cancer progression? *Biochem Mol Biol J* 1 (1) (2015).
- [12] J.H. Wei, J. Seemann, Unraveling the Golgi ribbon, *Traffic (Copenhagen, Denmark)* 11 (11) (2010) 1391–1400.
- [13] I. Cortesy-Theulaz, A. Pauloin, S.R. Pfeffer, Cytoplasmic dynein participates in the centrosomal localization of the Golgi complex, *J. Cell Biol.* 118 (6) (1992) 1333–1345.
- [14] T. Fujiwara, K. Oda, S. Yokota, A. Takatsuki, Y. Ikehara, Brefeldin A causes disassembly of the Golgi complex and accumulation of secretory proteins in the endoplasmic reticulum, *J. Biol. Chem.* 263 (34) (1988) 18545–18552.
- [15] J.F. Presley, N.B. Cole, T.A. Schroer, K. Hirschberg, K.J. Zaal, J. Lippincott-Schwartz, ER-to-Golgi transport visualized in living cells, *Nature* 389 (6646) (1997) 81–85.
- [16] K. Hirschberg, C.M. Miller, J. Ellenberg, J.F. Presley, E.D. Siggia, R.D. Phair, J. Lippincott-Schwartz, Kinetic analysis of secretory protein traffic and characterization of golgi to plasma membrane transport intermediates in living cells, *J. Cell Biol.* 143 (6) (1998) 1485–1503.
- [17] R. Pohlmann, G. Nagel, A. Hille, M. Wendland, A. Waheed, T. Bräulke, K. von Figura, Mannose 6-phosphate specific receptors: structure and function, *Biochem. Soc. Trans.* 17 (1) (1989) 15–16.
- [18] S. Nakagomi, M.J. Barsoum, E. Bossy-Wetzler, C. Sutterlin, V. Malhotra, S.A. Lipton, A Golgi fragmentation pathway in neurodegeneration, *Neurobiol. Dis.* 29 (2) (2008) 221–231.
- [19] S. Mukherjee, R. Chiu, S.M. Leung, D. Shields, Fragmentation of the Golgi apparatus: an early apoptotic event independent of the cytoskeleton, *Traffic (Copenhagen, Denmark)* 8 (4) (2007) 369–378.
- [20] C.M. McKinnon, H. Mellor, The tumor suppressor RhoBTB1 controls Golgi integrity and breast cancer cell invasion through METTL7B, *BMC Cancer* 17 (1) (2017) 145.
- [21] A. Petrosyan, C.A. Casey, P.W. Cheng, The role of Rab6a and phosphorylation of non-muscle myosin IIA tailpiece in alcohol-induced Golgi disorganization, *Sci. Rep.* 6 (2016) 31962.
- [22] D. Liazoghli, S. Perreault, K.D. Micheva, M. Desjardins, N. Leclerc, Fragmentation of the Golgi apparatus induced by the overexpression of wild-type and mutant human tau forms in neurons, *Am. J. Pathol.* 166 (5) (2005) 1499–1514.

- [23] G. Joshi, Y. Chi, Z. Huang, Y. Wang, A $\beta$ -induced Golgi fragmentation in Alzheimer's disease enhances A $\beta$  production, *Proc. Natl. Acad. Sci. U. S. A.* 111 (13) (2014) E1230–E1239.
- [24] W. Hu, R. Xu, G. Zhang, J. Jin, Z.M. Szulc, J. Bielawski, Y.A. Hannun, L.M. Obeid, C. Mao, Golgi fragmentation is associated with ceramide-induced cellular effects, *Mol. Biol. Cell* 16 (3) (2005) 1555–1567.
- [25] D. Jaarsma, C.C. Hoogenraad, Cytoplasmic dynein and its regulatory proteins in Golgi pathology in nervous system disorders, *Front. Neurosci.* 9 (2015) 397.
- [26] K. Suga, H. Hattori, A. Saito, K. Akagawa, RNA interference-mediated silencing of the syntaxin 5 gene induces Golgi fragmentation but capable of transporting vesicles, *FEBS Lett.* 579 (20) (2005) 4226–4234.
- [27] M.A. Puthenveedu, A.D. Linstedt, Evidence that Golgi structure depends on a p115 activity that is independent of the vesicle tether components giantin and GM130, *J. Cell Biol.* 155 (2) (2001) 227–238.
- [28] A.K. Gillingham, R. Sinka, L.L. Torres, K.S. Lilley, S. Munro, Toward a comprehensive map of the effectors of rab GTPases, *Dev. Cell* 31 (3) (2014) 358–373.
- [29] J. Shorter, R. Watson, M.E. Giannakou, M. Clarke, G. Warren, F.A. Barr, GRASP55, a second mammalian GRASP protein involved in the stacking of Golgi cisternae in a cell-free system, *EMBO J.* 18 (18) (1999) 4949–4960.
- [30] F.A. Barr, M. Puype, J. Vandekerckhove, G.J.C. Warren, GRASP65, a protein involved in the stacking of Golgi cisternae, *Cell* 91 (2) (1997) 253–262.
- [31] R. Duden, ER-to-Golgi transport: COP I and COP II function (Review), *Mol. Membr. Biol.* 20 (3) (2009) 197–207.
- [32] V. Belyy, M.A. Schlager, H. Foster, A.E. Reimer, A.P. Carter, A. Yildiz, The mammalian dynein–dynactin complex is a strong opponent to kinesin in a tug-of-war competition, *Nat Biol Cell* 18 (9) (2016) 1018.
- [33] J. Chia, G. Goh, V. Racine, S. Ng, P. Kumar, F. Bard, RNAi screening reveals a large signaling network controlling the Golgi apparatus in human cells, *Mol. Syst. Biol.* 8 (2012) 629.
- [34] B.A. Potter, R.P. Hughey, O.A. Weisz, Role of N- and O-glycans in polarized biosynthetic sorting, *Am. J. Phys. Cell Physiol.* 290 (1) (2006) C1–C10.
- [35] B. Hanßke, C. Thiel, T. Lübke, M. Hasilik, S. Höning, V. Peters, P.H. Heidemann, G.F. Hoffmann, E.G. Berger, K. von Figura, C. Körner, Deficiency of UDP-galactose:N-acetylglucosamine  $\beta$ -1,4-galactosyltransferase I causes the congenital disorder of glycosylation type IId, *J. Clin. Invest.* 109 (6) (2002) 725–733.
- [36] X. Ding, X. Jiang, R. Tian, P. Zhao, L. Li, X. Wang, S. Chen, Y. Zhu, M. Mei, S. Bao, W. Liu, Z. Tang, Q. Sun, RAB2 regulates the formation of autophagosome and autolysosome in mammalian cells, *Autophagy* (2019) 1–13.
- [37] X. Zhang, L. Wang, B. Lak, J. Li, E. Jokitalo, Y. Wang, GRASP55 Senses Glucose Deprivation through O-GlcNAcylation to Promote Autophagosome-Lysosome Fusion, *Dev. Cell* 45 (2) (2018) 245–261.
- [38] P. Ghosh, N.M. Dahms, S. Kornfeld, Mannose 6-phosphate receptors: new twists in the tale, *Nat. Rev. Mol. Cell Biol.* 4 (3) (2003) 202–212.
- [39] A. Adachi, F. Kano, T. Tsuboi, M. Fujita, Y. Maeda, M. Murata, Golgi-associated GSK3 $\beta$  regulates the sorting process of post-Golgi membrane trafficking, *J. Cell Sci.* 123 (Pt 19) (2010) 3215–3225.